

PHOTODISINTEGRATION OF SOME LIGHT NUCLEI AT INCIDENT
GAMMA RAY ENERGIES UP TO 40 MeV

M. TURK

Institute »Ruder Bošković« and University of Zagreb, Zagreb

Received 16 March 1976

Abstract: Several photonuclear reactions on ^{12}C and ^{14}N leading to three particles in the final state have been investigated using bremsstrahlung gamma rays from a 42 MeV betatron. Cross sections for reactions $^{12}\text{C}(\gamma, 3\alpha)$, $^{12}\text{C}(\gamma, p\alpha)^7\text{Li}$, $^{12}\text{C}(\gamma, d\alpha)^6\text{Li}$, $^{14}\text{N}(\gamma, 2\alpha)^6\text{Li}$ and $^{14}\text{N}(\gamma, {}^3\text{He}^4\text{He})^7\text{Li}$ are given as functions of gamma energy. Correlation measurements of some reactions at fixed excitation energy of the target nucleus show the predominance of sequential decays.

1. Introduction

Neutron induced kinematically complete experiments performed in nuclear emulsions have shown that various modes of interaction can be studied without complicated and expensive electronic equipment^{1,2}). By using gamma rays as incident radiation different decay modes can be studied on the same nuclei. In fact, since 1951 experiments on photodisintegration in nuclear emulsions have been carried out, however without the usefull representation in two dimensional diagrams. If the nuclear emulsion is bombarded with gamma rays up to 20 MeV the most abundant many particle reaction is $^{12}\text{C}(\text{gamma}, 3\alpha)$. This reaction has been investigated by several authors in various energy regions^{3,4}), the most thorough analysis with the greatest statistics being obtained by Toms³) who measured the reaction up to 20.5 MeV and also gave critical comparison of earlier results. Although most authors agree in the general appearance of the excitation curve, the absolute cross section varies considerably. The main source of discrepancy

seems to be the presence of other disintegrations in the emulsion. The separation of events is performed by using the momentum balance as the criterion of acceptability. If gamma rays are obtained from bremsstrahlung, as in most experiments they actually were, the continuous spectrum does not allow also the use of the energy balance — except in border cases when the calculated energy exceeds the peak energy of the source. Thus only reactions leading to charged particles can be studied. At energies up to 40 MeV several such reactions leading to three light charged particles in the final state may occur and they are listed below together with respective Q-values (in MeV)



Reactions of fairly less abundant isotopes of light elements in the emulsion have been omitted. Furthermore, only reactions with Q-values which allow a total kinetic energy release of more than 7 MeV have been listed. Measurements on reactions other than (1) were done by Maikov on reaction (2) at energies up to 80 MeV⁵⁾ and by Millard et al. on reaction (4) at 19–27 MeV⁶⁾.

The present experiment has been undertaken with the aim to measure the cross section for the reactions (1)–(5) up to 40 MeV incident energy and to study their modes of decay. Some preliminary results are given.

2. Experimental procedure

Nuclear emulsions have been irradiated by bremsstrahlung from a Siemens-Reiniger Werke 42 MeV betatron. With data supplied by the manufacturer the relative intensity spectrum has been estimated by comparison with the spectrum from a similar betatron operating at 35 MeV peak energy⁷⁾. These authors calculated the bremsstrahlung spectrum using Schiff's relations⁸⁾ and introduced corrections to obtain necessary agreement with experimental points. Their results have been extended to our case assuming the same dependence of the gamma intensity on the relative energy ν/ν_0 . The spectrum thus obtained is shown in Fig. 1 (dashed line). To eliminate low energy gamma rays causing fogging of the emulsion the bremsstrahlung beam was filtered through 40 cm of aluminium. The spectrum of the filtered beam is also plotted in Fig. 1 (solid line).

Ilford KO 200 μ thick plates were exposed to the filtered beam at 30° incident angle. Since the separation of various reactions depends on the accuracy

of measurement of momenta, the choice of emulsion type, time of exposure and the processing of the emulsion were adjusted to ensure the best measuring conditions in the microscope with reasonable density of events. Glycerine was added after processing to reduce the shrinkage and consequently the main cause of error in range measurements. However, the concentration of the glycerine-water solution has to be less than 5% because tracks of particles lighter than alpha can be lost as the density of grains reduces at higher doses of glycerine.

Altogether 1300 three prong stars have been found in 0,036 cc of emulsion. Measurements of track length and angle of emission were performed on each star and fed into a computer code. Energies and momenta of emitted particles were calculated on the assumption that each star could be produced by any of the possible reactions (1)–(5). In cases where the emitted particles are not identical permutations for a particular reaction have been computed, but only the one giving the minimum momentum imbalance was taken into further consideration.

The frequency distribution of the momentum imbalance for reaction (1) — $p(1)$ — has been plotted separately for each plate and each scanner. One typical distribution is shown in Fig. 2 (first diagram). Separate distributions have been drawn for the following groups of events:

- events with $p(1)$ significantly smaller than any $p(i)$ obtained on the basis of reactions other than (1);
- events with $p(1)$ significantly greater than any $p(i)$. The term «significantly» implies in these two cases that the absolute value of the difference, $\Delta p = |p(i) - p(1)|$, is larger than $0.7 \text{ (MeV}^{1/2} \text{ a. m. u.}^{1/2}\text{)}$;
- events where this difference is less than $0.7 \text{ (MeV}^{1/2} \text{ a. m. u.}^{1/2}\text{)}$.

It is obvious that the first and second group can be interpreted as comprising stars from reaction (1) and those representing the background, respectively. In the third group are those events which could not be assigned unambiguously to one or the other group. By comparing the three distributions for each set of data the final criterion for the separation of events has been determined.

A similar procedure has been adopted for other reactions, but a complete separation was not achieved, especially for stars with particles producing similar tracks in the emulsion, such as protons and deuterons (reactions (2) and (3)) or ^3He and alpha particles (reactions (4) and (5)). In these cases, overlapping events from the third group were given appropriate statistical weight.

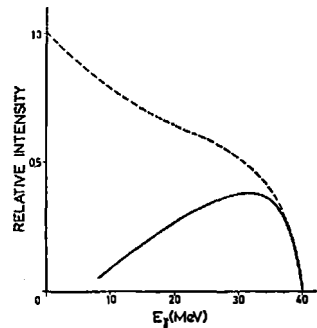


Fig. 1. Calculated gamma ray spectrum for unfiltered beam (dashed line) and for the beam filtered through 40 cm of aluminium (solid line).

The energy of the incoming gamma ray and the excitation energies for possible intermediate states were then computed for each event. All events from a particular reaction were sorted according to the computed gamma energy and

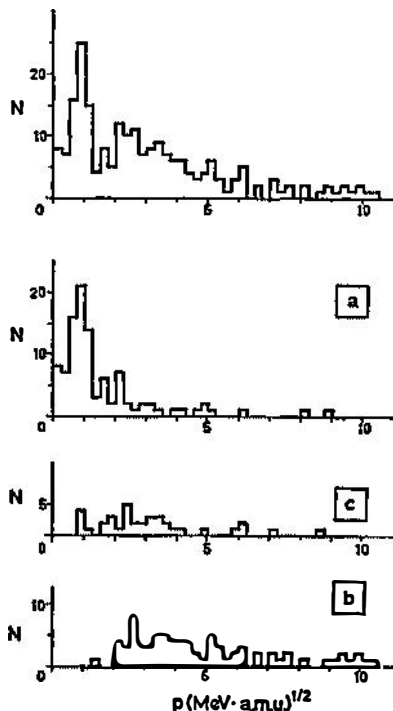


Fig. 2. The distribution of the momentum imbalance, $p(I)$, the latter calculated on the basis of reaction (1). The first diagram includes all events from a particular plate; (a)-events satisfying the momentum balance for reaction (1); (b)-events satisfying any of the reactions (2–5); (c)-events satisfying criteria for both groups.

excitation curves in a relative scale were obtained by dividing the number of events per 1 MeV energy interval by the corresponding gamma intensity from Fig. 1.

3. Results and discussion

Excitation curves. The excitation curve for the reaction $^{12}\text{C}(\gamma, 3\alpha)$ up to 20 MeV is shown in Fig. 3 with full points representing the results from the present experiment (bars are statistical errors). To obtain absolute cross sections the data have been normalized in this energy region where most previous experiments were performed. For reasons mentioned in the introduction our results have been fitted to Tom's data, points around 16–20 MeV with the greatest statistics being given maximum weight. The normalization factor was used to obtain the absolute cross section for other reactions. In Fig. 3 the results of other authors are represented by squares, the height of the square showing the spread of the data.

It must be pointed out that Tom's data are in the lower part of these squares, a fact to be borne in mind when comparison with earlier measurements is made at energies above 20 MeV.

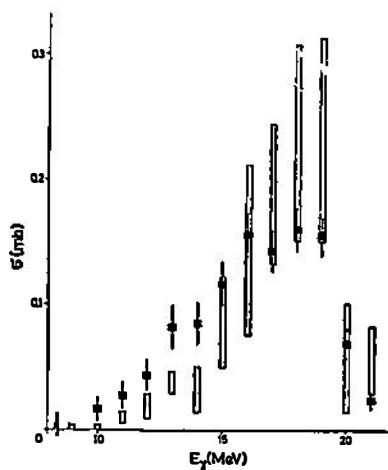


Fig. 3. Cross section for the reaction $^{12}\text{C}(\gamma, 3\alpha)$ as function of gamma ray energy after normalizing the data (full points) to Tom's results. Squares represent the spread of earlier measurements by various authors referenced in Ref. 3.

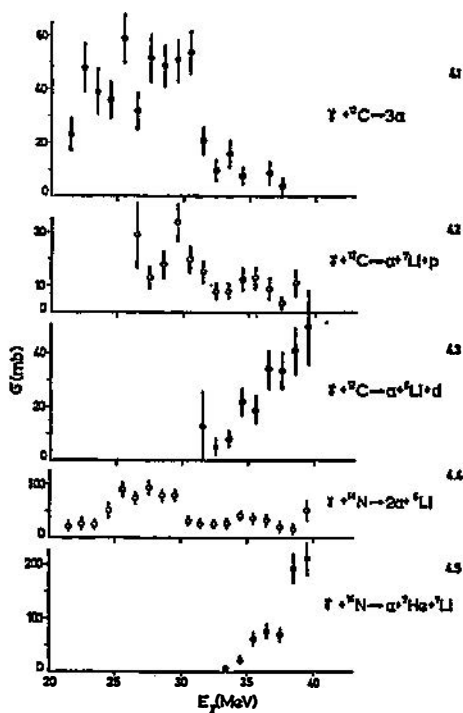


Fig. 4. Measured cross sections for reactions (1-5) as functions of incident gamma ray energy.

The excitation curves for all reactions listed in the introduction for $E_\gamma > 20$ MeV are shown in Fig. 4. In order to increase the statistics the cross section has been calculated in 1 MeV intervals which could have caused some smearing of the peaks. However, the graphs reproduce the overall variation of the cross section with gamma ray energy from threshold up to 40 MeV as well as the relative yield of various decays. The comparison of Fig. 4.1 and 4.3 indicates that the sudden decrease of the cross section for the decay of ^{12}C into 3 alpha particles at 30 MeV may be due to the competition of the $^{12}\text{C}(\gamma, d\alpha)^6\text{Li}$ reaction. The cross sections for reactions (2) and (3) have to be regarded as lower limits, because some events with more energetic light particles (p or d) may be missing due to the use of KO emulsions.

Comparison with other measurements shows no satisfactory agreement. This is not surprising as most of the measurements above 20 MeV were done by authors whose data do not agree with Tom's at lower energies. Furthermore, at higher energies, especially if the measurements are extended over 60 MeV the num-

ber of reactions combined with the wide range of possible values for the calculated gamma ray energy may cause serious overlapping of events. In his study of reaction (2) Majkov⁵⁾ did not take into account the possible contribution of reaction (3). Results on reaction (4) at energies 16–20 MeV⁶⁾, though larger than ours, are not in actual disagreement because of their large statistical errors.

Modes of decay. To study the modes of decay of the various reactions by means of two dimensional diagrams events corresponding to a particular excitation energy of the excited nucleus should be selected. However, in the projected spectrum all data from a particular reaction may be summed up, the peaks showing the overall appearance of an intermediate state in the sequential decay. For the three body decay of ^{12}C , which is known to be a sequential decay via excited states of ^8Be , Fig. 5 shows for all excitations of ^{12}C the characteristic ^8Be spectrum (each event being represented by three points, one »true« and two »spurious« ones): the narrow ground state, the broad 2.9 MeV state and events from the extremely broad 11.4 MeV state. However at ~ 17 MeV higher excited states also appear.

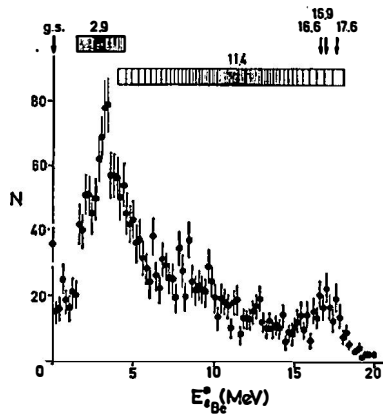


Fig. 5. ^8Be excitation energy distribution for all events from reaction $^{12}\text{C}(\gamma, 3\alpha)$. Squares show the width of levels at 2.9 and 11.4 MeV.

Some of the three particle decays of ^{14}N are represented in two dimensional Dalitz diagrams. Fig. 6 shows the reaction $^{14}\text{N}(\gamma, 2\alpha)^6\text{Li}$ in the $E_{10\text{B}}^*$ vs $E_{8\text{Be}}^*$ representation for $E_\gamma = (28.5 \pm 0.5)$ MeV. The diagram indicates that at this excitation energy the decay of ^{14}N into two alpha particles and ^6Li is a sequential process via the ^8Be nucleus, specifically the 2.9 MeV state and partly the 11.4 MeV state. The latter is almost outside the contour, but the decay is possible because this state is very broad. No decays via the intermediate nucleus ^{10}B have been found.

The reaction $^{14}\text{N}(\gamma, ^3\text{He}^4\text{He})^7\text{Li}$ is represented in the energy region $E_\gamma = (38.5 \pm 1.5)$ MeV. The events in the $E_{7\text{Be}}^*$ vs $E_{11\text{Be}}^*$ diagram show clustering of points along loci corresponding to excited states of ^{11}B (Fig. 7) — at 8.9-,

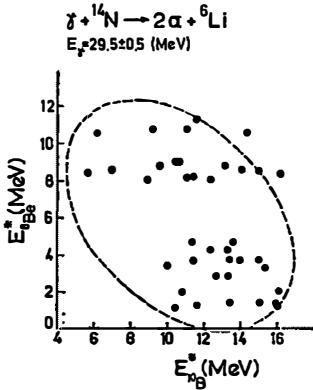


Fig. 6. $E_{10\text{B}}^*$ vs $E_{8\text{Be}}^*$ Dalitz diagram for the reaction $^{14}\text{N}(\gamma, 2\alpha)^6\text{Li}$ at $E_\gamma = (28 \pm 0.5)$ MeV.

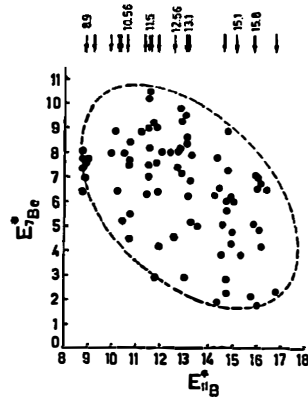
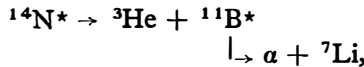


Fig. 7. $E_{11\text{B}}^*$ vs $E_{7\text{Be}}^*$ Dalitz diagram for the reaction $^{14}\text{N}(\gamma, ^3\text{He}^3\text{He})^7\text{Li}$ at $E_\gamma = (38.5 \pm 1.5)$ MeV.

10.5-, 11.5-, 13.1-, 15.1-, 15.8-, MeV — indicating that in this energy region reaction (5) proceeds predominantly via the sequential decay



where ^7Li must be left in the ground state, or, perhaps, the first excited state at 0.475 MeV, as the second excited state at 4.63 MeV is unstable to the α -t decay.

Acknowledgment

This experiment has been possible because the betatron facilities at the Central Institute for tumors in Zagreb have been extended to us. Special thanks are due to Mr. M. Bistrović for his cooperation. The author is indebted to Professor I. Šlaus for valuable suggestions.

References

- 1) B. Antolković, Nucl. Instr. Meth. **100** (1972) 211; Nucl. Phys. **A219** (1974) 332;
- 2) B. Antolković and Z. Dolenc, **A237** (1975) 235;
- 3) M. E. Toms, Nucl. Phys. **50** (1964) 561*);
- 4) J. P. Roalsvig, Can J. Phys. **43** (1965) 330;
- 5) V. N. Maikov, ŽETF **34** (1958) 1406;
- 6) C. H. Millar and A. G. W. Cameron, Can J. Phys. **31** (1953) 723;
- 7) H. Kulenkampff, M. Scheer, E. Schrüfer and J. Seyerlein, Naturwiss. **21** (1958) 509;
- 8) L. I. Schiff, Phys. Rev. **83** (1951) 252.

*1) and references within.

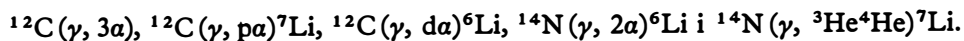
FOTODEZINTEGRACIJA LAKIH JEZGARA IZAZVANA γ ZRAKAMA ENERGIJE DO 40 MeV

M. TURK

Institut »Ruder Bošković i Sveučilište u Zagrebu, Zagreb

Sadržaj

Ispitivane su fotonuklearne reakcije sa tri nabijene čestice u konačnom stanju na lakim jezgrama. Korištene su gama zrake dobivene zakočnim zračenjem na betatronu maksimalne energije 42 MeV. Nuklearne emulzije Ilford KO služile su kao meta i detektor. Izmjereni su udarni presjeci u zavisnosti o energiji gama zraka za ove reakcije:



Korelaciona mjerenja vršena su za neke upadne energije na jezgri ^{14}N . Analiza pomoću Dalitzovih dvodimenzionalnih dijagrama pokazala je da je raspad ^{14}N na dvije alfa čestice i ^6Li pri upadnoj energiji 28.5 MeV sekvencijski proces preko ekscitiranih stanja 2.9 MeV i 11.4 MeV jezgre ^8Be .

U reakciji $^{14}\text{N}(\gamma, ^3\text{He}^4\text{He})^7\text{Li}$ pri 38.5 MeV pojavljuju se stanja intermedijarne jezgre ^{11}B .